Electronic Supplementary Material (ESI) for CrystEngComm.

Supporting Information:

Controllable Synthesis of Novel One-dimensional Structured ZIFs via the Supramolecular Self-assemblies

Yali Li[a], Jianhua Zhu[*a,b], Mingfang Cui [a], Jufen Yan[a]

[†]Anhui Province Key Laboratory of Metallurgical Emission Reduction & Resources Recycling. Anhui University of Technology.

[‡]Key Laboratory of Metallurgical Emission Reduction & Resources Recycling (Anhui University of Technology), Ministry of Education, Hudong Street 59, Maanshan, Anhui, China. E-mail: thesea@ustc.edu.cn. Fax: +86 0555-2311879. Phone: +86 0555-2311879.

Experimental section

Materials

Sodium cholate hydrate (SC, for cell culture, ≥99.0%), 2-Methylimidazole (MeIM, 98%) and Benzimidazole (BIM, AR, > 98.0%, GC) were purchased from Aladdin. N, N-Dimethylformamide (DMF, AR, 99.5%), Zinc acetate dihydrate ($Zn(COOH)_2 \cdot 2H_2O$, AR, 99.0%) and Cobalt nitrate hexahydrate ($Co(NO_3)_2 \cdot 6H_2O$, AR, 98.5%) were bought from Sinopharm Chemical Reagent Co., Ltd. Peroxidase from horseradish (HRP, RZ:>2.5, Freeze-dried powder, activity:>200 units/mg), Pyrogallic (>99.0%, GC) and Doxorubicin hydrochloride (DOX, 98%) were obtained from Aladdin. All chemicals were used without further modification. Stock solutions are prepared using Millipore water (18.2 mΩ•μs).

Preparation of ZnSC self-assemblies

ZnSC supramolecular assemblies were prepared by simply mixing isometric SC solution (50 mM) with $Zn(COOH)_2 \cdot 2H_2O$ solution (10 mM) with vigorously shaking for 2 seconds. Different amount of DMF was added into above solution to generate various templates. And then the mixed solution stand for 12h at 20±2℃.

Preparation of ZIF-8 microstructures

In a typical synthesis, the isometric MeIM (2.3 M) solution was gently added in as-prepared ZnSC (contained $[Zn]^{2+}$= 5 mM) self-assemblies without disturbances at 20± 2℃. The templates transcription process and the ZIF-8 growth process occurred simultaneously, with the deposition reactions on the surface of ZnSC self-assemblies. The final ZIF-8 products were collected by centrifugation and washed with ethanol for three times to removing the SC.

Doxorubicin loaded in ZIF-8 nanobelts (DOX/ZIF-8)

To remove the solvent, 100 mg of ZIF-8 solids were suspended into a 500 mL of deionised water 24h and after centrifugation. DOX was loaded in 5mg of ZIF-8 nanobelts by soaking in 2 mL of a DOX aqueous solution (2 mg/mL) for 24 hours. The impregnation was repeated two times. The DOX/ZIF-8 were recovered by centrifugation (10000 rpm, 10 min) and dried by freeze dryer. DOX was quantified by UV-vis spectrophotometer (emission maximum at 481 nm). Moreover, the loading capacity of DOX is defined as $(m_0-m_1)/m_S$, in which m_0 is the total mass of DOX, m_1 is the mass of DOX in the supernatant and m_S is the mass of the sample.

DOX delivery

The release of DOX was studied by suspending 5 mg of DOX/ZIF-8 materials in 4mL PBS (0.1M, pH 7.4). These suspensions were kept under fixed agitation and temperature (37℃) for different incubation times (from 30 min to 10 days). At each time point, an aliquot of 1 mL of supernatant solution was recovered by centrifugation (10000 rpm (5600 x g)/10 min) and replaced with the same volume of fresh PBS. The quantity of released DOX was measured by a UV-Vis spectrophotometer.

Cell cultures

Human hepatoma carcinoma cells (HEPG-2)(Cells Resource Center, Shanghai Institutes of Biological Science, China) were cultured in Dulbecco's modified Eagle's medium (DMEM) supplied with 10% fetal bovine serum (FBS) and 1% penicillin-streptomycin at 37℃ under a 5% CO_2 humidified atmosphere. Confluent cells were subcultured every 3 days using the standard procedure.

In vitro cytotoxicity tests

For the MTT (3-(4,5-dimethylthiazol-2-yl)-2,5-diphenyltetrazolium bromide) assay, HEPG-2 cells were seeded in 96-well plates at a proper concentration cells per well and cultured for 24 h. The sterilized samples of pure as-prepared ZIF-8 nanobelts or docetaxel-loaded ZIF-8 nanomaterials were added into the wells at concentrations ranging from 0.1 to 50 μg/mL and were co-cultured with the cells for 24 h. Cell viability was quantified by the MTT assay (at a wavelength of 490 nm), and each data was represented as the mean value of three parallel measurements. All reagents used in the cell viability experiments were purchased from Sigma-Aldrich. Optical images of the HEPG-2 cells co-cultured with different materials for 24 h were obtained using a confocal laser scanning microscope (Leica, SP8, Germany).

Synthesis of HRP@ZIF-8 composites

HRP-loaded ZIF-8 nanobelts were synthesized by weighing certain amount of ZIF-8 sample into HRP aqueous (1 mg/mL), followed by vigorous stirring for 24 hours at room temperature. The obtained precipitate was recovered by centrifugation at 5600 x g for 10 min. The encapsulation efficiency (47%) of HRP loaded in ZIF-8 materials was measured using UV-vis spectroscopy at 280 nm according to a pre-determined calibration curve. The calculation principle of encapsulation efficiency is referred to above DOX's.

Bioactivity of HRP@ZIF-8

The activity of HRP encapsulated in ZIF-8 micropores was determined by measuring the amount of decomposition of hydrogen peroxide with pyrogallol

converted to purpurogallin. In a typical assay, a moderate of ZIF-8/HRP crystals were added into a fixed solution containing 76 μL pyrogallol (5% w/w in deionized water), 38μL H_2O_2 (5% w/w in deionized water) and 1.8 mL of PBS buffer (pH 7.4). Immediately, the absorbance of the reaction solution was measured at 420 nm using a UV-Vis spectrophotometer at 30 s increments.

Characterizations

The morphology of products was observed by using a Hitachi S-4800 field-emission scanning electron microscope (FE-SEM). High-resolution transmission electron microscope photographs (HRTEM) were performed on a JEOL JEM 2011 microscope at an accelerating voltage of 200 kV. Energy-dispersive X-ray (EDX) spectroscopy measurements were carried out at 10 kV with the help of an installed Oxford INCA microanalysis system. The optical microscopy and polarized optical microscopy (POM) images were taken with a Leica microscope (DM 6000, German). XRD patterns were obtained on a Japan Rigaku Ultima IV X-ray diffractometer equipped with graphite-monochromatized Cu-*K*α radiation (λ=1.54178 Å). FT-IR spectra were measured on a Nicolet 6700 FT-IR using attenuated total reflection (ATR) method by SMART iTR (diamond). The thermal analysis was carried by Netzsc (STA 449 *F3*). The surface area and pore size distribution were calculated using the Brunauer–Emmett–Teller (BET) (V-sorb 2800MP, Gold APP Instrument Corporation China) method based on adsorption data. UV-vis absorption spectra were collected using a single beam spectrometer model SpectroVis Plus (Vernier Software & Technology, Beaverton OR, USA).

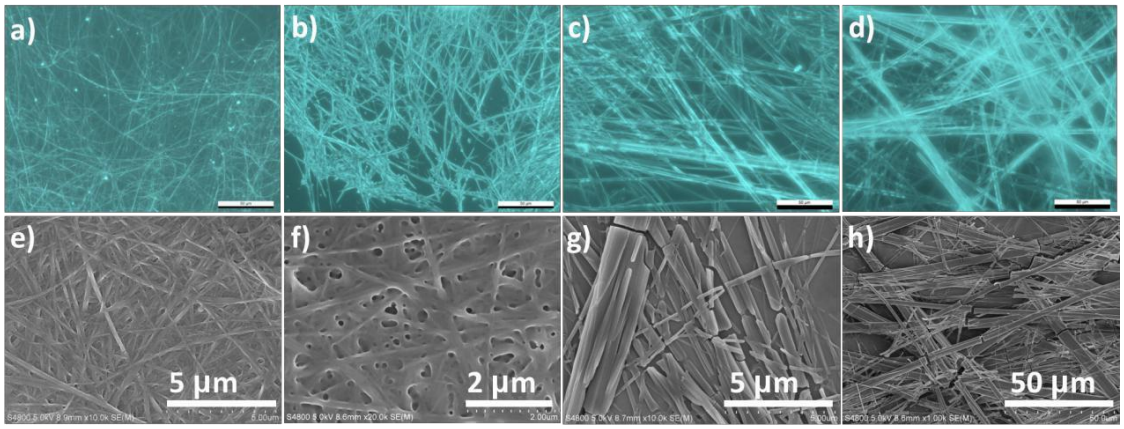

Fig. S1 Polarized optical microscopy (POM) images and SEM images of ZnSC templates. a, e) R= 0; b, f) R= 0.33; c, g) R= 0.8; d, h) R= 2.3.

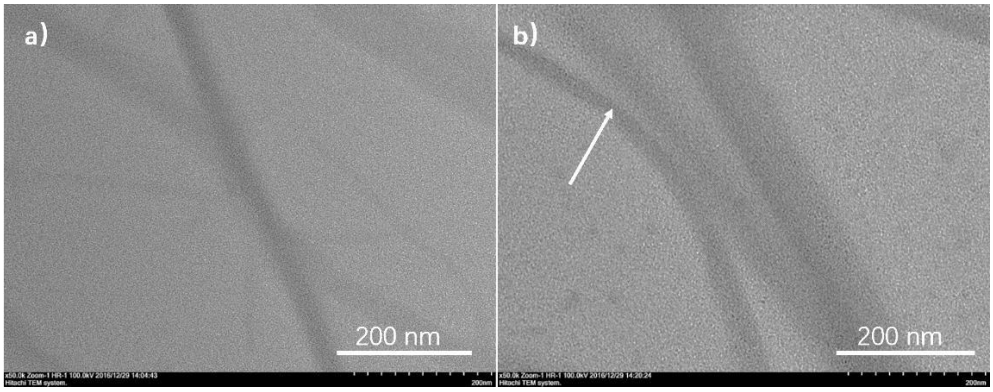

Fig. S2 TEM images of ZnSC ultrafine nanofibers obtained after (a) 0.5 and (b) 1h. R=0.33.

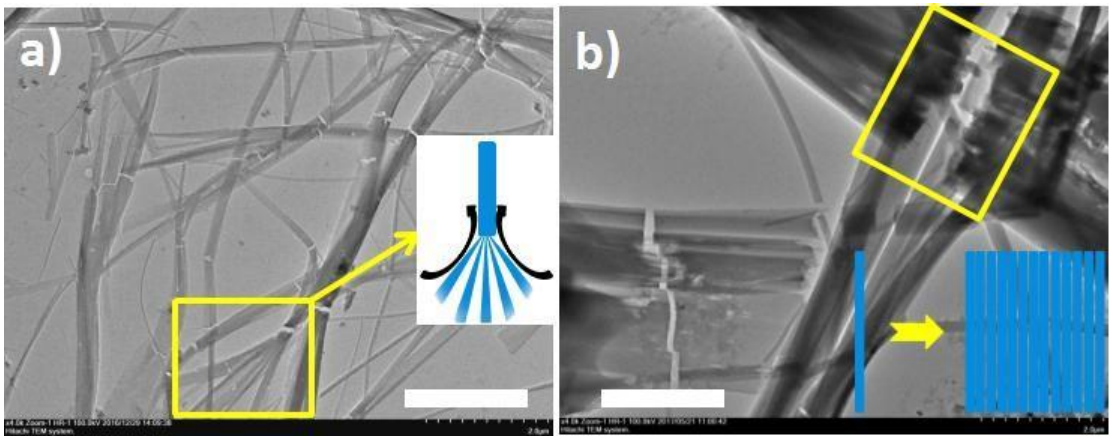

Fig. S3 TEM images of ZnSC obtained when R are 0.82(a) and 2.3(b) with incubated 1 hour. The scare bar is 2 μm.

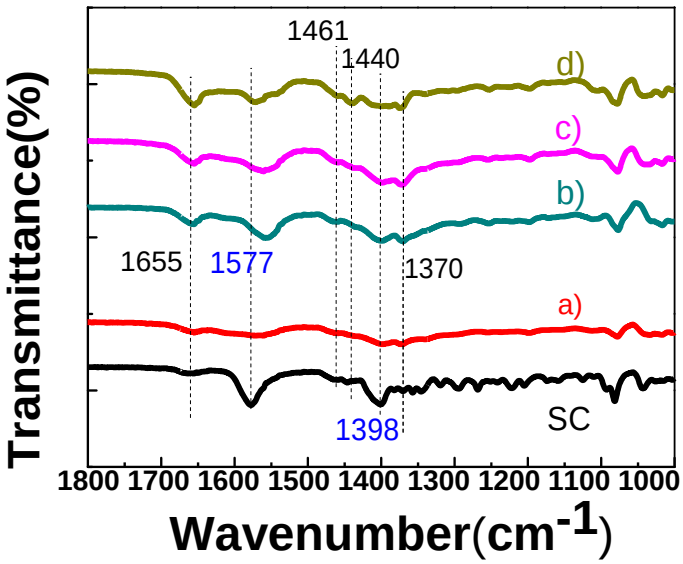

Fig. S4 FT-IR spectra of ZnSC nanofibers obtained at different R. a) 0. b) 0.33. c) 0.82. d) 2.3. T=20 ± 2℃.

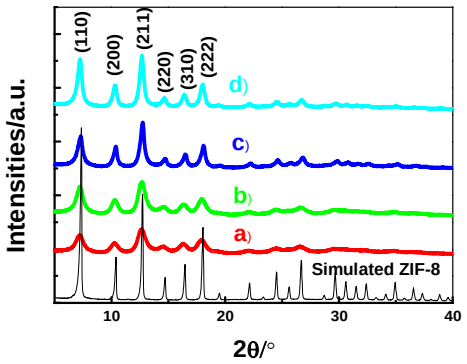

Fig. S5 XRD patterns of different ZIF-8 nanomaterials. a) Cross-linked ultrafine nanofibers. b) Nanotubes. c) Porous nanobelts. d) Helices.

Notes:

The reflection signals of all samples match well with the simulated powder XRD pattern of ZIF-8 single crystal, confirming the formation of ZIF-8 via the self-templates approach. Interestingly, the relative peak intensities, differ significantly when compared to that of the simulated pattern. Particularly, the peaks corresponding to {110} faces are relatively smaller.

It has been known that during the ZIF-8 crystallization, {100} faces of ZIF-8 initially grow fastest, which results into cubic subunits. And then the formation of 12 {110} faces dominates, which promotes the growth of truncatd rhombic dodecahedron single crystals. In our experiments, ZIF-8 clusters will initially deposit onto the templates. There has been no influence on the growth of {100} faces as the subunits are rather small in the early stage. However, the continuous growth of {110}

faces have been constricted in a certain degree possibly owing to the the crowded microenvironment on the templates.

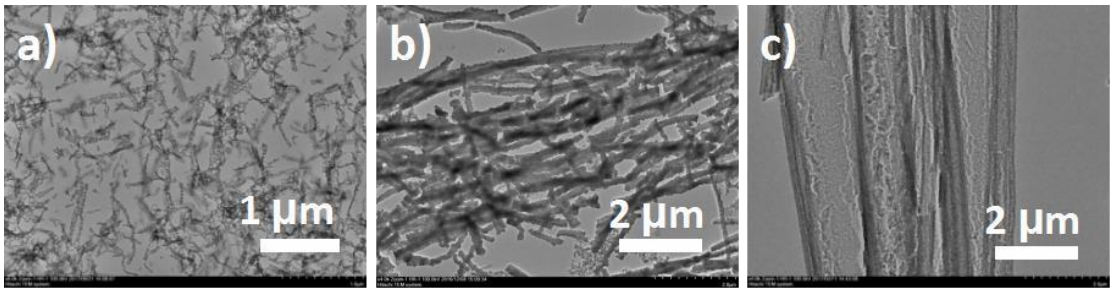

Fig. S6 TEM images of the resultant ZIF-8 developed from different ZnSC templates. a) Cross-linked nanofibers. b) Nanofibers. c) Porous nanobelts.

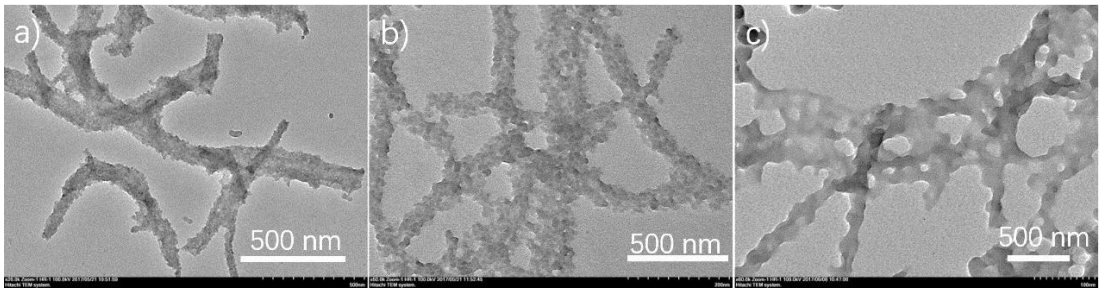

Fig. S7 TEM images of fibrous ZIF-8 nanostructures after different reaction time. a) 1h, b) 6h, c) 12h.

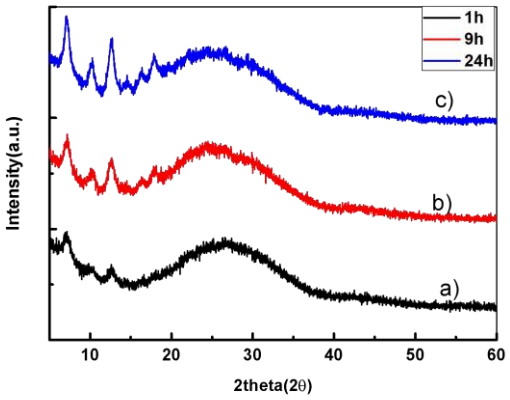

Fig. S8 XRD patterns of different ZIF-8 nanofibers in Fig. S6.

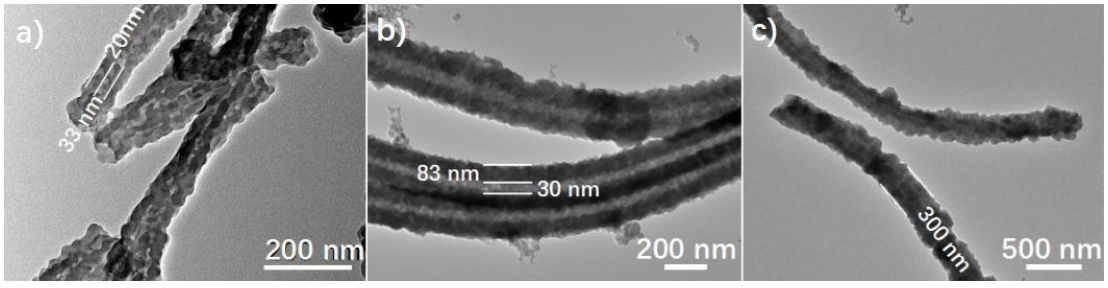

Fig. S9 TEM images of ZIF-8 nanotubes obtained at different time. a) 1h, b) 9h, c) 24h.

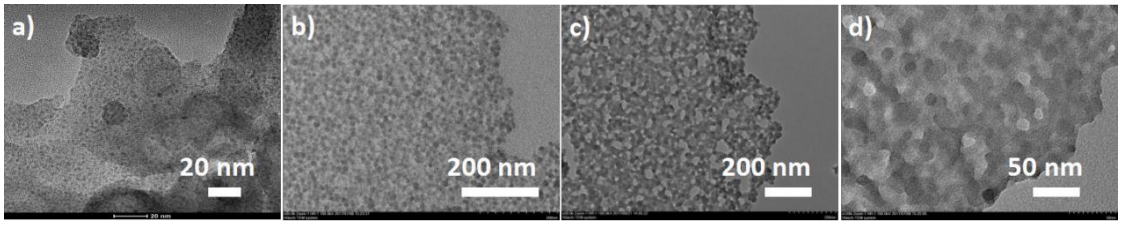

Fig. S10 TEM images of ZIF-8 nanobelts when prolonged the incubated time of ZIF-8 for a) 1h, b) 9h, c) 12h, d) 24h.

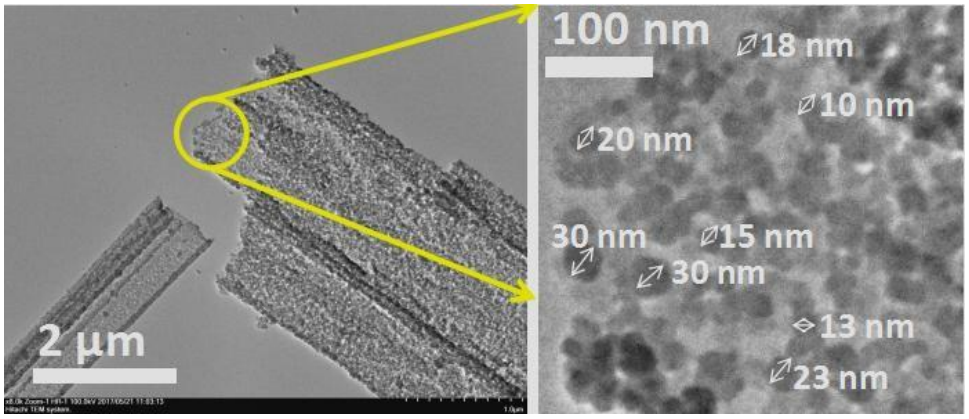

Fig. S11 TEM images of ZIF-8 nanobelts when MeIM with high concentrations (2.3 M). R= 2.3.

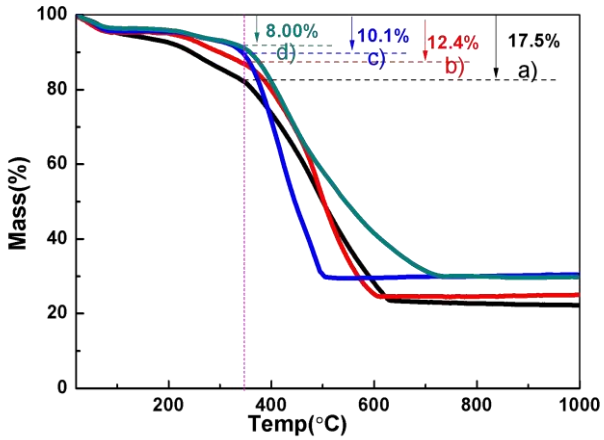

Fig. S12 The thermogravimetric curves of ZIF-8 samples. a) Cross-linked nanofibers. b) Nanotubes. c) Nanobelts. d) Nanohelices.

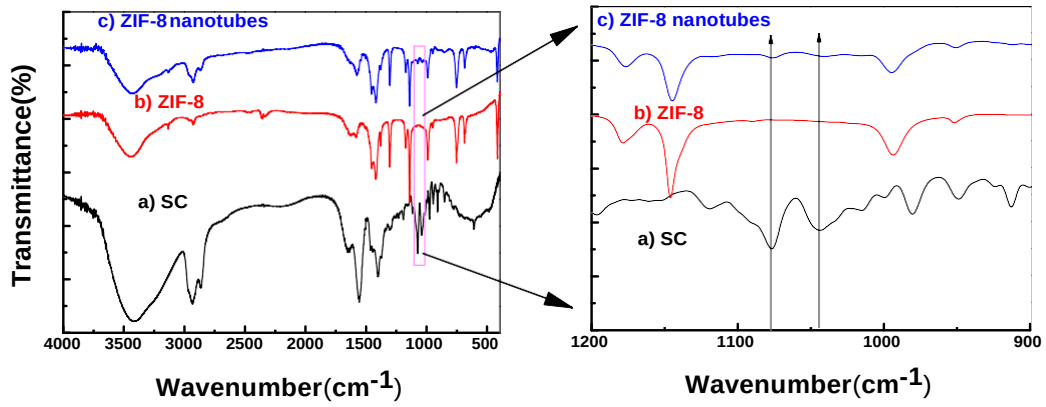

Fig. 13 FT-IR spectra of different samples. a) SC molecules, b) pure ZIF-8 materials and c) ZIF-8 nanotubes.

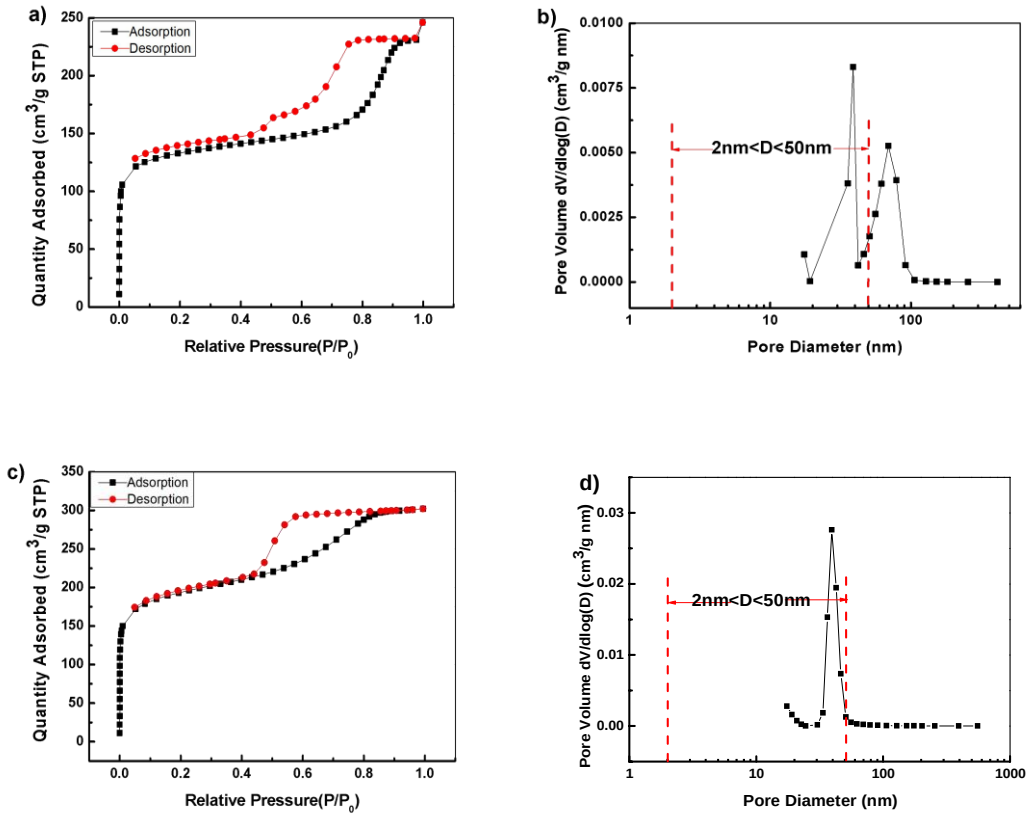

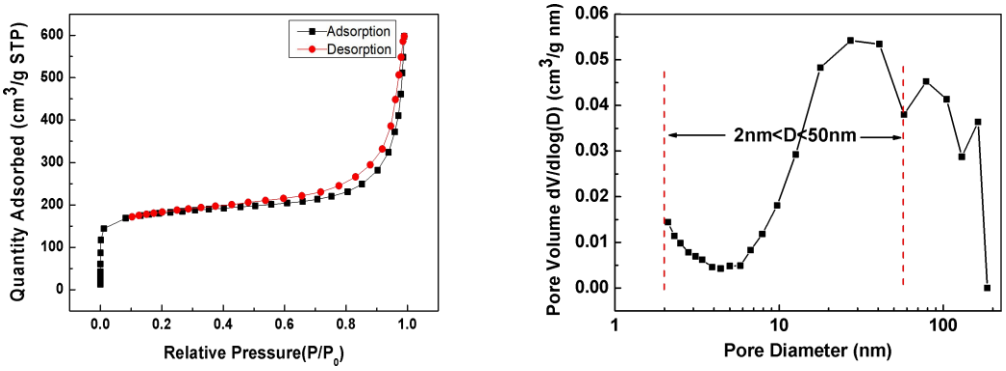

Fig. S14 N_2 adsorption-desorption isotherms of ZIF-8 a) Cross-linked nanofibers. c) nanotubes. e) Nanohelices. b), d) and f) represent the corresponding pore-size distributions using the Barett–Joyner–Halenda (BJH) method.

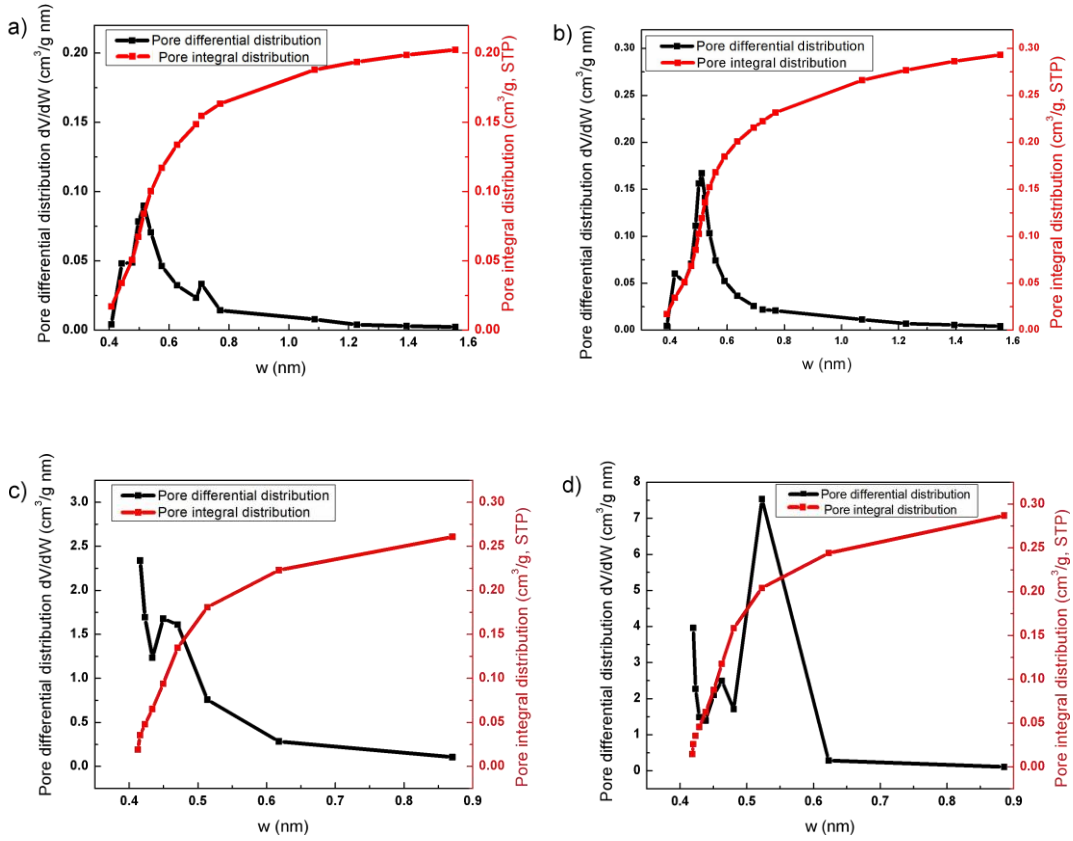

Fig. S15 Horvath-Kawazoe (HK) pore size distribution curves of a) Cross-linked ultrafine nanofibers. b) Nanotubes. c) Porous nanobelts. d) Helices.

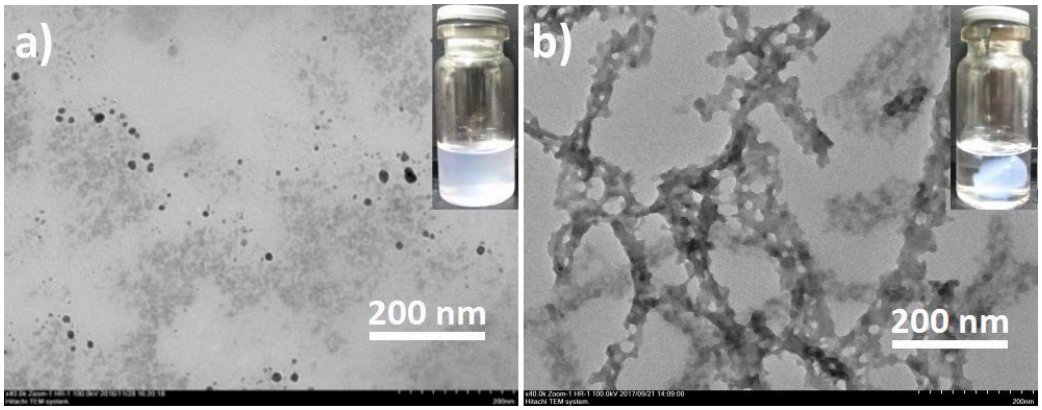

Fig. S16 TEM images of ZIF-8 obtained in (a) MeIM/NIW solution and (b) MeIM/DMF solution.

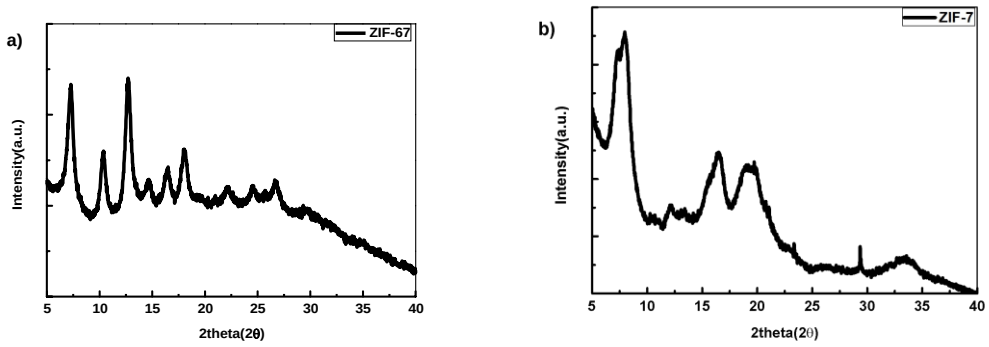

Fig. S17 XRD patterns of a) ZIF-67 and b) ZIF-7 nanomaterials.

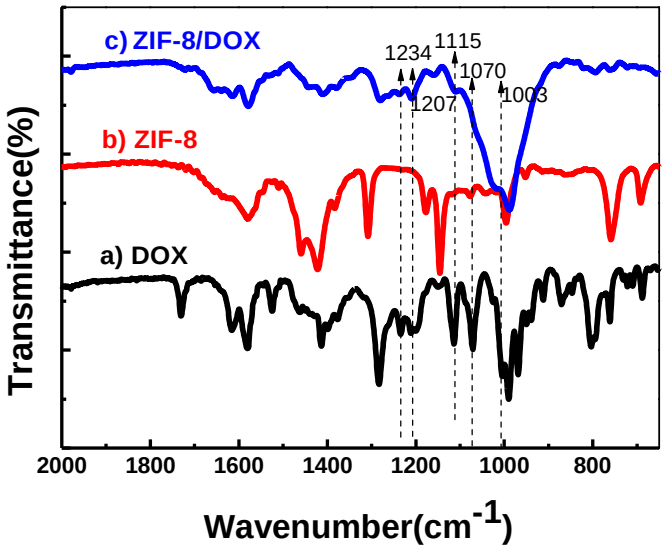

Fig. S18 FT-IR spectra of a) DOX drug, b) ZIF-8 nanobelts and c) ZIF-8/DOX.

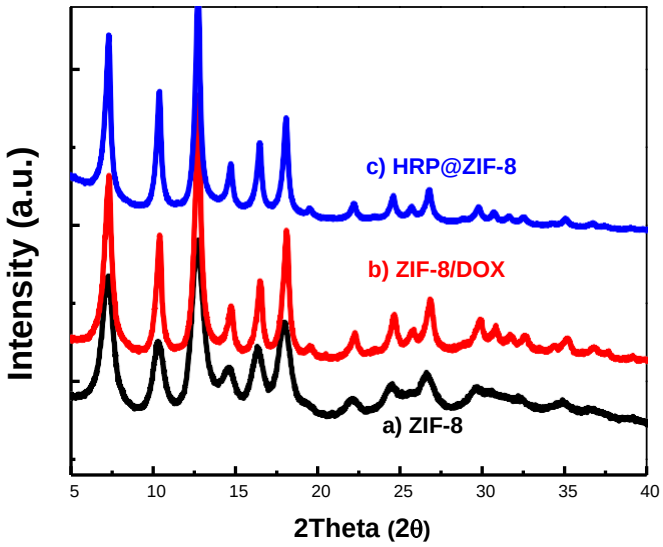

Fig. S19 XRD patterns of a) ZIF-8 nanobelts, b) ZIF-8/DOX and c) HRP@ZIF-8.

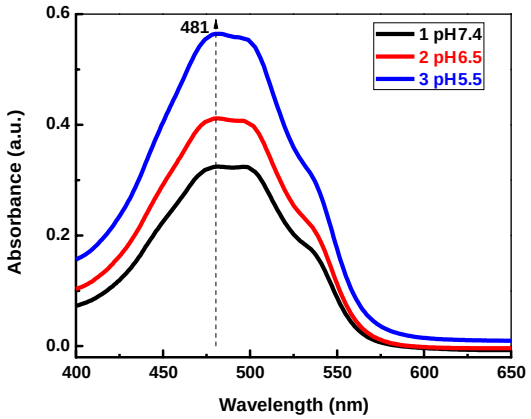

Fig. S20 UV-vis spectra of the released DOX from ZIF-8/DOX materials in various pH values of 7.4, 6.5, and 5.5. When the ZIF-8/DOX nanobelts were suspended in PBS solutions, the suspension solutions showed the featured absorption peak of DOX at 481 nm.

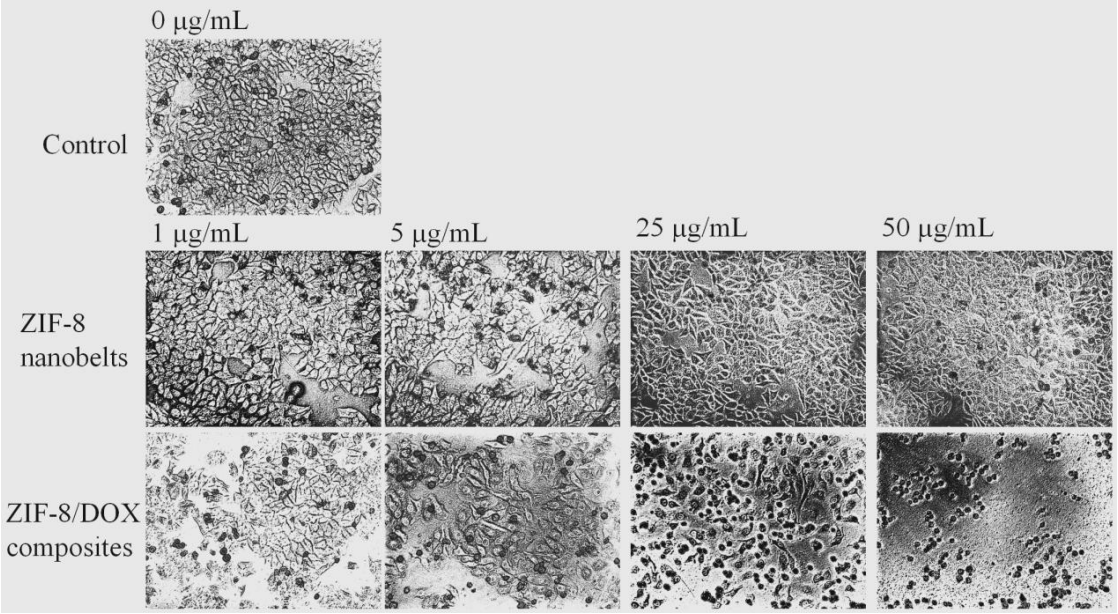

Fig. S21 The optical images of human hepatoma carcinoma cells (HEPG-2) without treated as a control at the first row, and were treated with different concentrations of pure ZIF-8 nanobelts without drug (the second row of images) and ZIF-8/DOX drug delivery system (the third row of images).

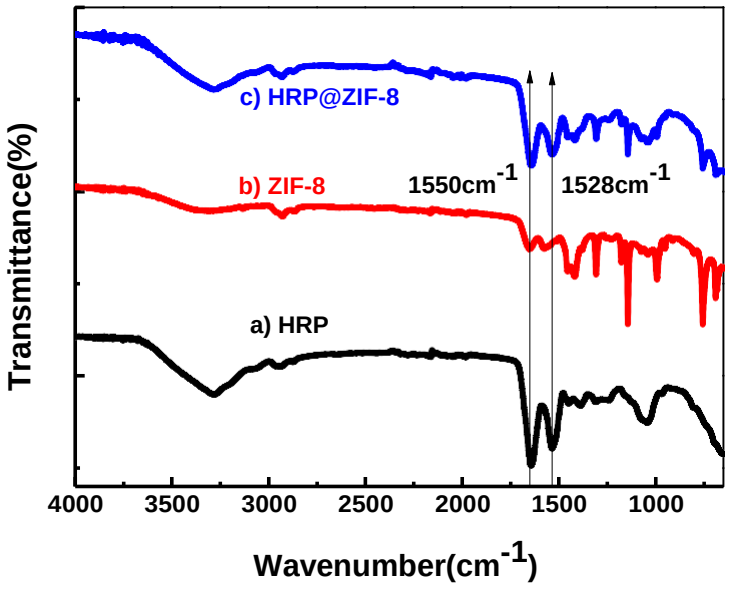

Fig. S22 FT-IR spectra of a) HRP, b) ZIF-8 nanobelts and c) HRP@ZIF-8.